FERMILAB-CONF-97/149-E

QCD RESULTS USING THE $k_\perp$ JET-FINDING ALGORITHM in $p\overline{p}$ COLLISIONS AT $\sqrt{s} = 1800$ GEV

D. Lincoln
University of Michigan, Ann Arbor, Michigan 48109, USA

(for the DØ Collaboration)

Abstract

An inclusive measurement of the jet mass as a function of jet $p_\perp$ has been made for jets with $|\eta| < 0.5$. This measurement is the first in a hadron collider environment using the $k_\perp$ jet-finding algorithm. This analysis shows that the HERWIG Monte Carlo well reproduces the average jet mass for high $p_\perp$ jets. At lower $p_\perp$, the data jets are 5–10% more massive. A second analysis has been performed with the same algorithm which measures the distribution of subjets (jets within jets).

The $k_\perp$ jet-finding algorithm [1], first proposed in 1990 [2], is based on the relative transverse momentum ($k_\perp$) of two partons, particles, or calorimeter towers. It has been used by the various LEP experiments to probe their jet physics [3]. This jet finding algorithm is considered by theorists to be more tractable than the usual cone [4] and JADE-style [5] algorithms. The areas in which this algorithm performs better than conventional algorithms are in low-$p_\perp$ jet reconstruction, dealing with jets which are close enough that their particles are extensively intermingled and jet structure measurements. For instance, the $k_\perp$ algorithm has been used by OPAL [3] to characterize the differences between quark and gluon jets. Such a study is expected to be undertaken by DØ. With the substantially larger $p_\perp$ range accessible at the Tevatron, DØ should be able to probe many different mixtures of quark and gluon jets.

Thus the study of jet characteristics is very vigorous. It is important that DØ use its excellent calorimetry and solid angle coverage to contribute to these studies, extending the measurements to higher $p_\perp$ and over a greater η range. This paper discusses two measurements: (a) an inclusive measurement of the mass (or width) of central jets as a function of $p_\perp$ and (b) a study of jet shapes.

The $k_\perp$ algorithm must be modified to be used in the hadron-hadron environment and proceeds via the following steps:

1. For each pair of particles, we calculate the function

$$d_{i,j} = \min(E_{\perp,i}^2, E_{\perp,j}^2)\frac{(\Delta\eta_{i,j}^2 + \Delta\phi_{i,j}^2)}{D^2} \tag{1}$$

   where D is a cut-off parameter and which is of order 1. Then we define

$$d_i = {E_{\perp,i}}^2. \tag{2}$$

2. The minimum $d_{\min}$ of all the d_i and $d_{i,j}$ is found.

3. If $d_{\min}$ is a $d_{i,j}$, then particles i and j are merged into a new, pseudo-particle k using one of a number of possible recombination schemes (outlined below). After recombination, both i and j are removed from the list of particles and d_{kl} is calculated for all $l \neq k$.

4. If $d_{\min}$ is a d_i (i.e. $\Delta\eta^2 + \Delta\phi^2 > D^2$ for all j), then the particle is not "mergeable" and it is removed from the list of particles and placed in a list of jets.

5. Return to step (1).

Steps (1-5) are repeated until all particles have been assigned to a jet. One is left with a list of jets. This list may be quite long and the jets with small $E_\perp$ can be thought of as soft radiation or belonging to the beam jets.

When two particles are merged, the kinematics of the resulting pseudo-particle is determined by summing their four-momenta. This choice is not unique, but is required for most jet structure studies.

One of the convenient features of the $k_\perp$ algorithm is that it is easy to generalize to the task of finding sub-jets (i.e. 'jets within jets'), which are expected to reflect the post-collision parton shower. While the $k_\perp$ algorithm discussed above is being run, a record is kept of which particles are included in which jet. The algorithm is run again on those particles contained in a jet, this time the quantity

$$y_{i,j} = \frac{\min(E_{\perp,i}^2, E_{\perp,j}^2)}{E_{\perp,\mathrm{jet}}^2} \frac{(\Delta\eta^2 + \Delta\phi^2)}{D^2} \tag{3}$$

is calculated. The process is iterated as described above and stopped when all $y_{i,j} > y_{\mathrm{cut}}$. What is left is a list of sub-jets. When $y_{\mathrm{cut}} = 0$, each particle is individually considered to be a subjet. When $y_{\mathrm{cut}} = 1$, one finds explicitly 1 subjet (i.e. the entire jet is the only subjet). Thus the number of subjets as a function of y_{cut} is a sensitive measure of jet structure.

In leading order calculations, jets have no internal structure, as each jet contains a single parton. In next-to-leading order calculations, it is possible that the various jet-finding algorithms can combine more than one parton into a jet. In a hypothetical full calculation, or in data, many particles are contained in a typical jet. When the energy and momentum of the jets are determined by the prescription discussed above, the condition $E \geq |p|$ must hold, implying that $E_\perp \neq |p_\perp|$. In the results presented here, $p_\perp = \sqrt{p_x^2 + p_y^2}$ is used. This E, p imbalance allows the mass of a jet to be defined.

$$m_{\mathrm{jet}} = \sqrt{E_{\mathrm{jet}}^2 - p_{\mathrm{jet}}^2} \tag{4}$$

For fixed jet $p_\perp$ and for $\Delta\eta \ll 1$ & $\Delta\phi \ll 1$, it can be shown [6] that the mass of a jet is proportional to the RMS width of a jet (in $\eta\phi$ space) and thus is a measure of physics accessible only in higher order calculations.

The first analysis presented here is a measurement of the jet mass as a function of the jet $p_\perp$. The data set includes 94 pb^{-1} of data recorded during the 1994–1996 Tevatron run. The hardware triggers considered were very loose, requiring only a $p\overline{p}$ collision and a large, local transverse energy deposition within the calorimeter. A higher threshold on the highest reconstructed $p_\perp$ jet was imposed to ensure the triggers were efficient. The measurement was essentially inclusive: the jets were ordered in $p_\perp$ and the eight highest $p_\perp$ jets were considered. Cuts requiring (1) a vertex within fifty centimeters of the nominal and (2) that no additional soft $p\overline{p}$ interactions occurred in the same beam crossing were imposed. Jet quality cuts were imposed on the event to remove spurious jets. If any of the jets in the event failed these cuts, the entire event was discarded. All jets in events passing these cuts, which also had $|\eta_{\mathrm{jet}}| < 0.5$, were accepted.

In order to understand the effects of the detector and errors in energy assignment, a Monte Carlo based on the HERWIG [7] and GEANT [8] packages was used. Events were generated without HERWIG's conventional underlying event and the detector response was then simulated. To each event, a minimum bias data event was added. This addition was intended to simulate the underlying event, along with uranium noise always present in the detector. Corrections were determined which corrected the measured jets back to the particle level jets. By definition, the particle level jets include only particles from the hard scatter and do not include particles from the underlying event. Differences in calorimeter response between the data and Monte Carlo were taken into account. The jet $p_\perp$ correction was approximately 15%. The jet mass correction was approximately 5% and was slightly dependent on jet $p_\perp$.

Figure 1 shows jet mass as a function of jet $p_\perp$ for both the corrected data and HERWIG at the particle level. HERWIG well reproduces the data at higher $p_\perp$ but systematically predicts less massive jets at low $p_\perp$. The systematic error is dominated by slight differences between the different jet ranks (highest $p_\perp$ jet is jet 1, second highest is jet 2, etc.)

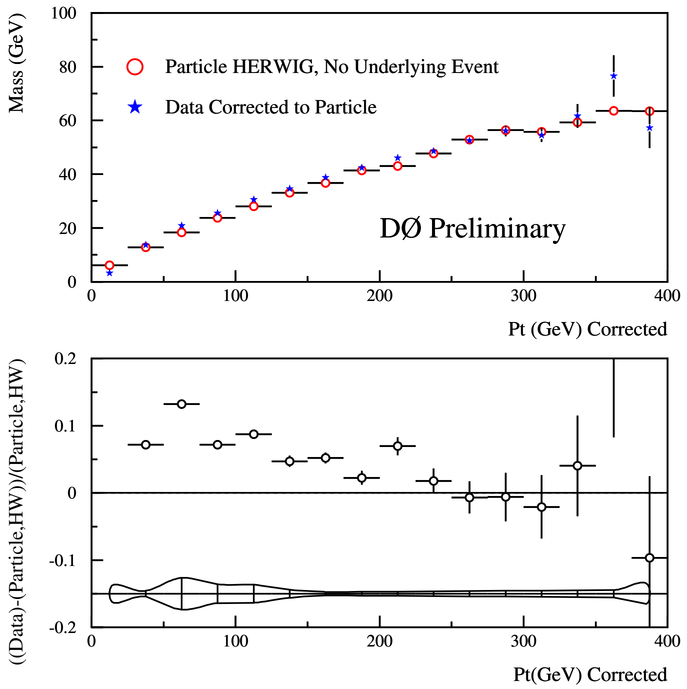

Figure 1: Top plot shows jet mass as a function of $p_\perp$ for both corrected data and HERWIG. The bottom plot shows the normalized ratio. The bottom band denotes the systematic error.

The second analysis explores the subjet structure (or lumpiness) of jets. In addition to the above described cuts, the jet $p_\perp$ was restricted ($275 < p_\perp^{\mathrm{jet}} < 350$ GeV) in order to restrict the scope of study and explore jets which should be better described by perturbative techniques.

Two particular results are shown here. In fig. 2, the average number of subjets $< N_{\rm subjet} >$ is given as a function of $y_{\rm cut}$. As expected, $< N_{\rm subjet} > = 1$ when $y_{\rm cut} \sim 1$, and increases as $y_{\rm cut}$ is lowered. In addition, HERWIG results are shown at the parton, particle and detector level. When detector response is included, the data is well reproduced by the Monte Carlo. The figure clearly shows that the detector response affects the measurement more than the fragmentation model.

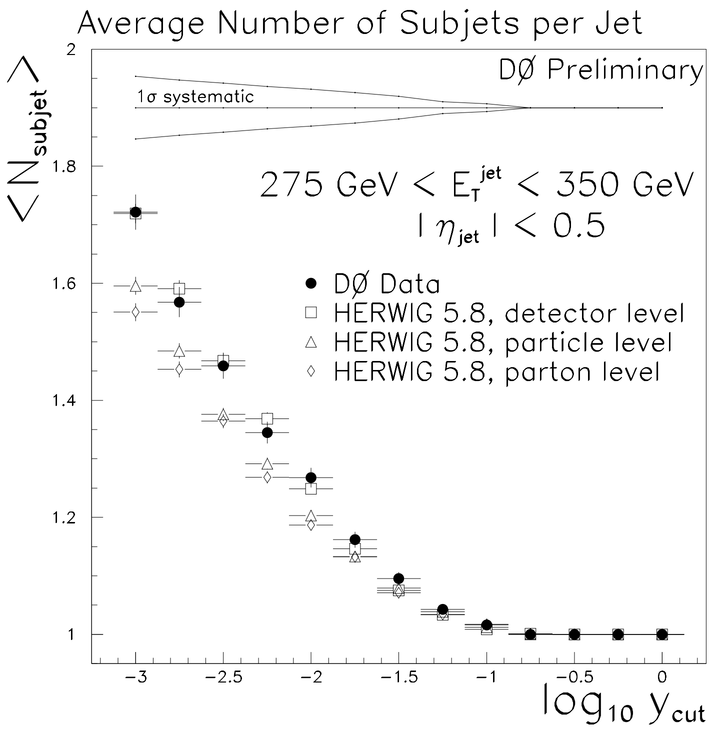

Figure 2: Average number of subjets as a function of the scale variable $y_{\rm cut}$.

If one chooses a particular probe scale (i.e. $y_{\rm cut}$), one can explore how the subjets are distributed within a (η, ϕ) cone of $R = 1$. This quantity is quantified by measuring the integrated $p_\perp$ contained within a cone centered on the jet axis.

$$< \rho(\Delta R) > \; = \frac{\sum p_\perp^{\rm subjet}(\leq \Delta R)}{\sum p_\perp^{\rm subjet}(\leq 1.0)} \qquad (5)$$

As shown in fig. 3, one sees that these high $p_\perp$ jets are highly collimated, with 90% of the $p_\perp$ contained within a cone of radius 0.2. These results complement earlier studies [9].

To recapitulate, the $k_\perp$ jet finding algorithm has been implemented in a hadron collider environment. Preliminary results indicate that the structure of high $p_\perp$ is well reproduced by the HERWIG Monte Carlo. Additional studies intended to investigate more subtle features of jet structure are underway.

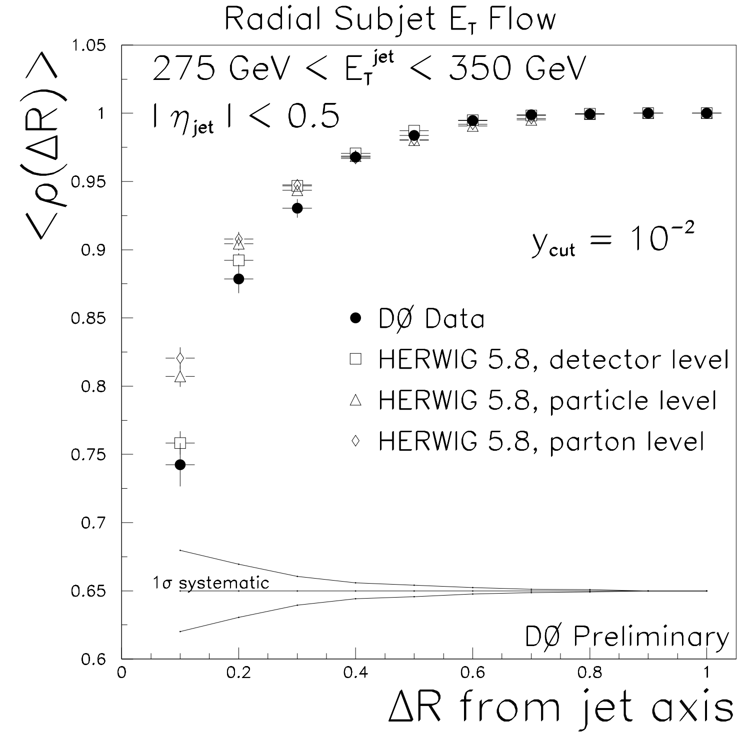

Figure 3: Average $p_\perp$ flow as a function of distance from the center of the jet.

References

[1] N. Brown and W. J. Stirling, Z. Phys. C 53 (1992) 629; S. Catani et al., Phys. Lett. B 285 (1992) 291; S. Catani et al., Nucl. Phys. B 406 (1993) 187; S. Ellis and D. Soper, Phys. Rev. D 48 (1993) 3160.

[2] J. Phys. G: Nucl. Part. Phys. 17 (1991).

[3] G. Alexander et al., Z. Phys. C69 (1996) 543; R. Akers et al., Z. Phys. C68 (1995) 179; R. Akers et al., Z. Phys. C63 (1994) 363; G. Alexander et al., Phys. Lett. B265 (1991) 462.

[4] J. Huth, et al., FERMILAB-CONF-90-249-E, Snowmass Summer Study 1990, p. 134-136.

[5] W. Bartel et al., Zeit. Phys. **C33** (1986) 23; S. Bethke et al., Phys. Lett. B 213 (1988) 235.

[6] D. Lincoln, DØNote #2998, Unpublished.

[7] G. Marchesini et al., Comput. Phys. Commun. 67 (1992) 465.

[8] R. Brun, Geant3 Users Guide, CERN DD/EE/84-1 (1987).

[9] S. Abachi et al., Phys. Lett. B, **357**, 500, (1995).